Peierls Transition with Acoustic Phonons and Solitwistons in Carbon Nanotubes

Marc Thilo Figge, Maxim Mostovoy, and Jasper Knoester
Institute for Theoretical Physics and Materials Science Center, University of Groningen, Nijenborgh 4, 9747 AG Groningen, The Netherlands
(Received 5 September 2000)

We show that the Peierls instability can result in softening of acoustic phonons with small wave vectors and suggest that this unusual transition takes place in carbon nanotubes, resulting in a static twist deformation of the nanotube lattice. The topological excitations in the ordered phase are immobile and propagate only in pairs.

DOI: 10.1103/PhysRevLett.86.4572 PACS numbers: 63.20.Kr, 05.45.Yv, 63.70.+h, 72.80.Rj

Phase transitions involving phonon softening caused by an electron-lattice instability, occur in many kinds of crystalline solids, e.g., ferroelectrics, Jahn-Teller systems, and charge- and spin-density-wave materials. The nature and wave vector $\mathbf{q}$ of the soft phonon depends on the mechanism of the structural transition. For instance, the charge redistribution within unit cells of ferroelectric materials results in the softening of acoustic phonons with small $\mathbf{q}$, manifest in the vanishing of the phonon velocity v at the transition temperature [1]. On the other hand, for the charge- and spin-density-wave transitions in metals with nested Fermi surfaces, $\mathbf{q}$ equals the nesting vector [2]. Thus, in quasi-one-dimensional Peierls materials the strong mixing of low-energy particle-hole excitations and phonons with $q = 2k_F$ (k_F is the Fermi wave vector), causes the frequency of these phonons to vanish at the transition temperature. At half filling, this leads to a semiconducting state in which the lattice sites are alternatively displaced to the left and to the right, thereby doubling the lattice period (lattice dimerization) [3].

In this Letter we show that, surprisingly, also acoustic phonons may soften due to a Fermi surface instability. In particular, we show that in a half-filled metallic carbon nanotube (CNT) the Peierls mechanism of the metal-insulator transition does not increase the lattice period but, instead, forces the nanotube to twist around its axis. We estimate the transition temperature and discuss the effect of the instability on the conductivity of the tubes. We also introduce and derive the properties of a new type of elementary excitation: *solitwistons,* which are kinks in both the twist angle and the lattice dimerization.

An undoped CNT of the armchair type is a half-filled quasi-one-dimensional conductor [4]. The conduction electrons have zero momentum around the CNT circumference. The Fermi surface consists of two points, $k = \pm k_F$, with k the electron wave vector along the CNT axis. As the CNT unit cell contains two C ions (Fig. 1), two bands of electrons with velocities $\pm v_F$ cross at each Fermi point (Fig. 2). The Hamiltonian describing the electrons near the Fermi surface, i.e., valid close to half filling, has the form

$$H_{\mathrm{el}} = \sum_{n,\sigma} \int dx\, \Psi^{\dagger}_{n\sigma}(x)\, \frac{v_F}{i}\, \hat{\sigma}_3\, \frac{\partial}{\partial x}\, \Psi_{n\sigma}(x)\,. \qquad (1)$$

Here, $\hat{\sigma}_3$ is the Pauli matrix and we set $\hbar = 1$. The spinor $\Psi_{n\sigma} = \binom{\psi_{Rn\sigma}}{\psi_{Ln\sigma}}$ denotes electrons moving to the right/left with Fermi velocity v_F near the Fermi point $n = 1, \ldots, N_F$ (for the CNT, $N_F = 2$).

As is clear from Fig. 2, two types of electron backscattering (reverting the sign of the electron velocity) occur in the armchair CNT. The dashed arrow indicates the usual backscattering, taking place between two different Fermi points. The relevant short-wavelength phonons correspond to the Kekulé structure of the CNT. In addition, however, a second type of backscattering exists, which is caused by long-wavelength phonons and leaves the electron near the same Fermi point (solid arrow). In what follows we will solely concentrate on the latter type of backscattering, as it leads to a new type of Peierls distortion and topological excitation. We have checked that inclusion of the first type of backscattering does not suppress this instability; in fact, it even increases its critical temperature.

The hexagonal lattice of the cylindrically shaped CNT is composed of two triangular sublattices $i = A, B$, distinguished by open and closed circles in Fig. 1. The vector $\vec{r} = (x, y)$ describes the coordinates of C ions along and perpendicular to the CNT axis, whereas the vector

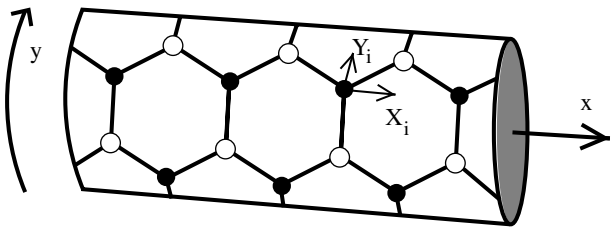

FIG. 1. Schematic picture of an armchair CNT. The open and closed circles denote the C ions of the two triangular sublattices $i = A, B$. Also indicated are the definitions of the lattice displacements.

 0031-9007/01/86(20)/4572(4)$15.00

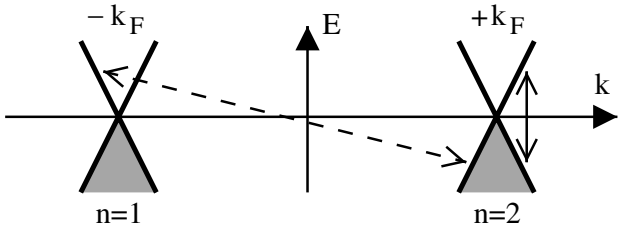

FIG. 2. Electron energy dispersion near the Fermi energy of a half-filled armchair CNT and the two types of backscattering processes distinguished in the text.

$\vec{R}_i(\vec{r}) = (X_i, Y_i)$ describes the shifts of the ions. Since the transverse momentum of the electrons near the Fermi surface is zero, the relevant ionic displacements depend only on the x coordinate along the CNT axis: $\vec{R}_i = \vec{R}_i(x)$. The lattice is invariant under the reflection in the plane containing the CNT axis (P_y): $y \to -y$, $X_A \leftrightarrow X_B$, $Y_A \leftrightarrow -Y_B$, and in the plane perpendicular to the axis (P_x): $x \to -x$, $X_i \to -X_i$, $Y_i \to Y_i$. The general expression for the lattice Hamiltonian of the long-wavelength phonons compatible with the symmetries of the lattice is

$$H_{\text{lat}} = \frac{1}{2}\int dx[\rho_x(\dot{X}_+^2 + \dot{X}_-^2) + \rho_y(\dot{Y}_+^2 + \dot{Y}_-^2) + \alpha_x X_-^2 + \alpha_y Y_-^2 + \beta_x X_+'^2 + \beta_y Y_+'^2 + \gamma_x X_-'^2 + \gamma_y Y_-'^2 + 2\delta_x X_- Y_+' + 2\delta_y Y_- X_+'] . \tag{2}$$

Here, $X_\pm = (X_A \pm X_B)/\sqrt{2}$ and $Y_\pm = (Y_A \pm Y_B)/\sqrt{2}$, while the prime and the dot denote, respectively, spatial and time derivatives. The constants ρ_x, ρ_y are the mass densities, while the other parameters are the harmonic lattice constants. The four phonon modes can be classified by their parity P_y. The acoustic and optical positive parity modes, for which $X_- = Y_+ = 0$, correspond to a relative motion of the two sublattices in the circumferential direction. As the corresponding lattice distortions do not affect the length of the bonds along the CNT axis, these modes result only in forward scattering and are discarded below. On the other hand, the two negative parity modes ($X_+ = Y_- = 0$), one optical ($\omega_o = \sqrt{\alpha_x/\rho_x}$) and one acoustic [$\omega_a(q) = v_0|q|$ with $v_0 = \sqrt{(\alpha_x\beta_y - \delta_x^2)/(\rho_y\alpha_x)}$], correspond to an alternation of bond lengths along the CNT axis, which results in electron backscattering.

Assuming that the electron hopping depends on the distance between neighboring sites, the Hamiltonian describing the electron backscattering off the negative parity phonons with small phonon momenta q has the form

$$H_{\text{el-lat}}[\Delta_o + \Delta_a] = \sum_{n,\sigma}\int dx\, \Psi_{n,\sigma}^\dagger(\Delta_o + \Delta_a)\hat{\sigma}_1\Psi_{n,\sigma}\,, \tag{3}$$

where $\hat{\sigma}_1$ is the Pauli matrix, while Δ_o and Δ_a are the fields describing the optical and acoustic phonons, respectively, with $P_y = -1$:

$$\begin{cases} \Delta_o = c_o(X_- + \frac{\delta_x}{\alpha_x}Y_+')\,, \\ \Delta_a = -c_a Y_+'\,, \end{cases} \tag{4}$$

where $c_o \simeq 3\alpha_\parallel/\sqrt{N_c}$ and $c_a = c_o(4\delta_x + d\alpha_x)/(4\alpha_x)$ contain the electron-lattice coupling $\alpha_\parallel$, the number N_c of zigzag chains around the circumference of the armchair CNT, and the distance d between two carbon atoms in the undistorted hexagonal lattice. In terms of the fields Δ_a and Δ_o, the lattice Hamiltonian (2) decouples:

$$H_{\text{lat}} = \sum_{j=o,a}\left[\frac{N_F}{\pi\lambda_j v_F}\int dx\,\Delta_j^2 + \frac{\rho_j}{2c_j^2}\int dx\left(\frac{\partial\Delta_j}{\partial t}\right)^2\right]. \tag{5}$$

Here, ρ_j is the mass density ($\rho_o = \rho_x, \rho_a = \rho_y$) and the dimensionless coupling constant $\lambda_j = N_F c_j^2/(\pi v_F \rho_j f_j^2)$, with $f_o = \omega_o$, for the optical phonon, and $f_a = v_0$, for the acoustic phonon. From Eq. (4) we see that to lowest order in the derivatives, the optical phonon corresponds to a relative shift of the triangular sublattices along the nanotube axis (X_-), while the acoustic phonons describe a twist distortion of the cylindrical CNT lattice (Y_+). Both modes result in a lattice deformation with out-of-phase bond length dimerization in neighboring zigzag chains along the CNT axis.

For $\Delta_a = 0$ and $N_F = 1$, the Hamiltonian of our model, given by the sum of Eqs. (1), (3), and (5), coincides with the TLM model of *trans-polyacetylene* [5]. On the other hand, for $\Delta_o = 0$ and $N_F = 2$, it becomes the Hamiltonian describing the electron-twiston interactions, which was used to explain the linear temperature dependence of the resistivity of the armchair CNTs [6].

Phase transition.—First we consider the temperature dependence of the optical and acoustic phonon frequencies for $T > T_c$. The coupling of the phonons to electrons mixes the bare optical and acoustic phonon modes and renormalizes their frequencies. The renormalized optical phonon frequency, $\tilde{\omega}_o(q)$, obtained in the random phase approximation, is for $\tilde{\omega}_o(q) \ll T$ given by (cf. Ref. [2])

$$\tilde{\omega}_o^2(q) = \omega_o^2(q)[1 - \lambda_o \ln(\gamma W/\pi T)], \tag{6}$$

while it is hardly affected for $\tilde{\omega}_o(q) \gg T$. Here W is the energy cutoff of the order of the electron band width and $\gamma = 1.781\,072\ldots$ is the exponential of the Euler's constant. Similarly, the renormalized acoustic phonon frequency, $\tilde{\omega}_a(q)$, is found to be

$$\tilde{\omega}_a^2(q) = \omega_a^2(q)\,\frac{1 - (\lambda_o + \lambda_a)\ln(\gamma W/\pi T)}{1 - \lambda_o \ln(\gamma W/\pi T)}\,. \tag{7}$$

In deriving Eq. (7) we assumed that $\tilde{\omega}_a(q) \ll T, \tilde{\omega}_o(q)$.

We thus see that $\tilde{\omega}_o(q)$ is independent of λ_a and is the same as in the absence of the coupling to acoustic phonons. On the other hand, the renormalized acoustic phonon frequency depends on the sum of λ_a and λ_o. As a result, the acoustic phonons "soften" first, at the critical

temperature which follows from Eq. (7) to be given by

$$T_c = \frac{\gamma}{\pi} W \exp\left(-\frac{1}{\lambda_a + \lambda_o}\right). \quad (8)$$

As $\tilde{\omega}_a(q = 0) = 0$ at all temperatures, the "softening" in this case means vanishing of the acoustic phonon velocity at $T = T_c$. Thus, no matter how much λ_o is larger than λ_a, it is always the velocity of the acoustic phonon that becomes zero at the transition temperature, whereas the optical phonon frequency stays finite at $T = T_c$. This is a consequence of the mixing of the optical and acoustic phonons due to their interactions with electrons, which results in a repulsion between the frequencies of the two modes. As a result, the optical and acoustic branches can never cross and the singularity at T_c always occurs in the lower, i.e., acoustic, branch.

The Peierls transition in metallic CNTs has been considered in previous studies where, however, only the interaction between electrons and a single optical phonon mode has been taken into account [7]. Our model also includes acoustic phonons, which are coupled to optical ones through excitation of virtual electron-hole pairs. Therefore, in this model the average values of both Δ_a and Δ_o become nonzero below the transition temperature T_c. In the mean-field treatment of the lattice one has to minimize the total free energy with respect to the two order parameters Δ_a and Δ_o. The solutions of the resulting self-consistency equations have the following properties: (i) The Bogoliubov–de Gennes equations for the sum of the optical and acoustic order parameters, $\Delta(x) = \Delta_o(x) + \Delta_a(x)$, are the same as in the TLM model with a single phonon mode [5] and a degeneracy of the electronic states $N_d = 2N_F$, but with the coupling constant $\lambda = \lambda_o + \lambda_a$. (ii) The optical ($j = o$) and acoustic ($j = a$) order parameters are proportional to $\Delta(x)$: $\Delta_j(x) = (\lambda_j/\lambda)\Delta(x)$.

Thus the classical configurations minimizing the free energy of our model in the ordered state are identical to those for the TLM model. In particular, we obtain that the order parameter in the homogeneous state $\Delta(x) = \Delta_0$ at zero temperature has the value $\Delta_0 = (\pi/\gamma)T_c$, with T_c as in Eq. (8). As follows from Eq. (4), the nanotube in the ordered state is uniformly dimerized due to the relative shift, X_-, of the two triangular sublattices. This corresponds to the "frozen" optical phonon mode in the conventional Peierls scenario. In addition, however, below T_c the lattice develops a uniform twist, which corresponds to a linearly growing amplitude, $Y_+ \propto x$, of ionic displacements in the direction perpendicular to the CNT axis. Such a lattice distortion is not a frozen phonon mode, as it corresponds to large deviations of ions from their equilibrium positions in the high-temperature phase. The twist angle is proportional to the acoustic order parameter $\Delta_a = (\lambda_a/\lambda)\Delta_0$.

Topological excitations.—The topological excitations in the TLM model are kinks, or domain walls, in the order parameter. The analytical expression for the kink is given by $\Delta(x) = \Delta_0 \tanh(x/\xi_0)$, where $\xi_0 = v_F/\Delta_0$ is the correlation length [5]. Using this form of the kink and Eq. (4), we immediately arrive at the lattice distortions for a topological excitation in the CNT:

$$\begin{cases} X_-(x) \propto \Delta_0 \tanh(\frac{x}{\xi_0}), \\ Y_+(x) \propto -\Delta_0 \ln\cosh(\frac{x}{\xi_0}). \end{cases} \quad (9)$$

Near the kink both $\Delta_o(x)$ and $\Delta_a(x)$ change sign and the combination of a dimerization kink (soliton) and a change in the sign of the twist angle suggests to call this topological excitation a solitwiston.

Because of the internal degeneracy $N_d = 4$, the solitwiston's spin-charge relations coincide with those of the kink in polyyne [8]: In the (undoped) armchair CNT the neutral solitwiston ($Q = 0$) can have spin $S = 0$ or $S = 1$ since two electrons occupy the midgap states at the two Fermi points. If one electron is removed from (added to) the system, the corresponding charged solitwiston is found to have charge $Q = +e$ ($Q = -e$) and spin $S = 1/2$, while for two removed (added) electrons the doubly charged solitwiston has spin $S = 0$. Thus, in contrast to the exotic spin-charge relations of solitons in *trans-polyacetylene,* those relations are quite usual for the solitwistons in CNTs. The TLM model also describes a nontopological polaronic excitation corresponding to a bound solitwiston-antisolitwiston pair [5]. For CNTs we call this excitation a *polartwiston,* as it describes a local indentation of both the optical and acoustic order parameter.

Since, according to Eq. (4), in the ordered state, X_- is of the same order as dY'_+, one may doubt the validity of the continuum approximation used above. Therefore, we also performed numerical calculations of the optimal lattice configuration at $T = 0$. For this purpose we considered an elastic spring model, including harmonic interactions between C ions up to the third neighbor. We used a steepest-descent algorithm to determine the minimal energy lattice configuration of the CNT. The values of the coupling parameters involved were chosen to satisfy two conditions: (i) The correlation length, ξ_0, is much smaller than the system size. (ii) The coupling between the shifts Y_+ and X_- is small, so that approximately $\Delta_o \propto X_-$, while $\Delta_a \propto Y'_+$. The numerical results for periodic boundary conditions on the shifts are shown in Fig. 3. At half filling (a), we obtain $Y_+ = 0$ and a finite value for X_-, corresponding to a relative shift of the two triangular sublattices A and B. The absence of a twist in the ground state, which is in obvious contradiction with the result of the continuum approximation, is a finite-size effect: The uniform twist is simply incompatible with the periodic boundary conditions for the given CNT length and model parameters.

In (b) we show the effect of doping on the lattice configuration (a) by adding $N_{\mathrm{el}} = 1, \ldots, 4$ electrons to the initially half-filled system. For an additional electron the creation of a polaronic excitation is, in principle, energetically more favorable than the creation of a solitwiston.

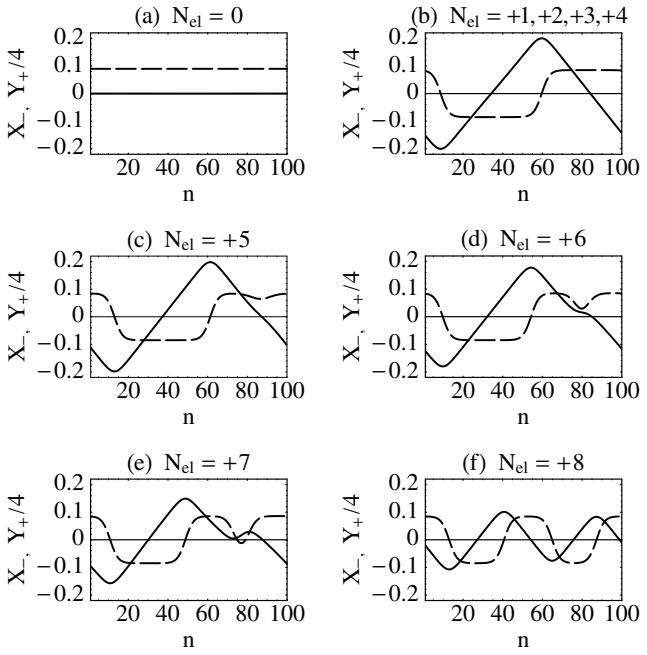

FIG. 3. Peierls state of the armchair CNT for periodic boundary conditions imposed on the shifts X_- (dashed line) and Y_+ (solid line). The index $n = 1, \ldots, 100$ denotes rings of carbon atoms along the CNT axis (corresponding to 50 hexagons) and N_{el} denotes the number of added electrons.

However, since in the finite chain (a) there is no twist at half filling, the energy is minimized by creation of a solitwiston-antisolitwiston pair (b). As the antibonding superposition of the midgap states of the two solitwistons can accommodate up to $N_d = 4$ electrons, the lattice configuration (b) remains the same for $N_{\mathrm{el}} = 2$, 3, and 4. Then, on adding the fifth up to seventh electron, a charged polartwiston appears in the CNT lattice [see (c)–(e)]. This excitation distorts the lattice locally with an indentation of the order parameters that depends on the number of added electrons, similar to the polaron in polyyne [8]. Finally, we plot in (f) the minimal energy lattice configuration obtained with eight extra electrons for which the periodic boundary conditions require a second solitwiston-antisolitwiston pair to appear.

The creation energy of a solitwiston is $\mu = 4\Delta_0/\pi$, which is twice that of a soliton in the TLM model, due to the degeneracy $N_d = 4$ of the electronic states. The dynamical properties of the solitwistons, however, differ much more dramatically from those of the soliton in the TLM model. While in the latter the soliton can propagate along the chain without changing its profile, the shift of the solitwiston brings the entire CNT into motion and results in a constant kinetic energy density at distances larger than ξ_0 from the solitwiston position. Thus the mass of the solitwiston is proportional to the tube length, rendering isolated solitwistons immobile. They may, however, propagate in pairs, as such a motion only affects the ions between the two solitwistons. The mass of such a pair is proportional to the pair size.

Conclusions.—In this Letter, we studied the Peierls transition due to the backscattering of electrons on both optical and acoustic phonons. We found that, independent of the electron-phonon coupling constants, the acoustic phonon softens at T_c, whereas the optical phonon frequency remains finite. We suggest that such a transition takes place in armchair CNTs, leading to a static twist of the CNT below T_c. The topological excitations in our model are, unlike solitons in *trans-polyacetylene,* immobile and can propagate only in pairs. Since the coupling constant $\lambda \propto \frac{1}{N_c}$, where N_c is the number of zigzag chains around the CNT circumference, the critical temperature Eq. (8) decreases exponentially with N_c. As a result, the Peierls transition can take place only in small-radius nanotubes. We estimate $T_c \sim 10$ K for CNTs with $N_c = 8$ [9]. CNTs with small radius may also be of interest for technological applications [10] and examples of such small tubes have in fact been synthesized [11]. We note that due to the softening of the acoustic phonons (the twistons), the temperature dependence of the electrical resistivity calculated within our model shows a low-temperature upturn, which qualitatively agrees with experimental data on CNTs [6,9]. As twist deformations in CNTs have recently been observed using scanning tunneling microscopy [12], one may also speculate on the possibility to observe doping-induced solitwistons using this technique.

We gratefully acknowledge financial support by the Stichting Fundamenteel Onderzoek der Materie (FOM).

[1] M. J. Harris *et al.,* Phys. Rev. Lett. **71**, 2939 (1993).
[2] G. Grüner, *Density Waves in Solids* (Addison-Wesley, New York, 1994).
[3] R. E. Peierls, *Quantum Theory of Solids* (Clarendon, Oxford, 1955).
[4] For a review, see R. Saito, G. Dresselhaus, and M. S. Dresselhaus, *Physical Properties of Carbon Nanotubes* (Imperial College Press, London, 1998).
[5] H. Takayama, Y. R. Lin-Liu, and K. Maki, Phys. Rev. B **21**, 2388 (1980).
[6] C. L. Kane and E. J. Mele, Phys. Rev. Lett. **78**, 1932 (1997); C. L. Kane *et al.,* Europhys. Lett. **41**, 683 (1998); H. Suzuura and T. Ando, Mol. Cryst. Liq. Cryst. **340**, 731 (2000).
[7] K. Tanaka *et al.,* Int. J. Quantum Chem. **63**, 637 (1997); Y. Huang *et al.,* Solid State Commun. **97**, 303 (1996); K. Harigaya and M. Fujita, Phys. Rev. B **47**, 16 563 (1993); R. Saito *et al.,* Phys. Rev. B **46**, 1804 (1992); J. W. Mintmire, B. I. Dunlap, and C. T. White, Phys. Rev. Lett. **68**, 631 (1992).
[8] M. J. Rice *et al.,* Phys. Rev. B **34**, 4139 (1986).
[9] M. T. Figge, Ph.D. thesis, University of Groningen, 2000.
[10] A. A. Farajian, K. Esfarjani, and Y. Kawazoe, Phys. Rev. Lett. **82**, 5084 (1999).
[11] L. F. Sun *et al.,* Nature (London) **403**, 384 (2000).
[12] W. Clauss *et al.,* Phys. Rev. B **58**, R4266 (1998).